Separation Science and Technology
Publication details, including instructions for authors and subscription information:
http://www.informaworld.com/smpp/title~content=t713708471

CO_2 absorption into w/o emulsion with aqueous amine liquid droplets

Sang-Wook Park[a]; Hyun-Bum Cho[a]; In-Joe Sohn[a]; Hidehiro Kumazawa[b]
[a] Department of Chemical Engineering, Pusan National University, Pusan, Korea [b] Department of Chemical and Biochemical Engineering, Toyama University, Toyama, Japan

Online publication date: 23 April 2002

SEPARATION SCIENCE AND TECHNOLOGY, 37(3), 639–661 (2002)

CO_2 ABSORPTION INTO W/O EMULSION WITH AQUEOUS AMINE LIQUID DROPLETS

Sang-Wook Park,[1,*] Hyun-Bum Cho,[1] In-Joe Sohn,[1] and Hidehiro Kumazawa[2]

[1]Department of Chemical Engineering, Pusan National University, Pusan 609-735, Korea
[2]Department of Chemical and Biochemical Engineering, Toyama University, Toyama 930-8555, Japan

ABSTRACT

Rates of CO_2 absorption into aqueous droplets of monoethanolamine (MEA), diethanolamine (DEA), and triethanolamine (TEA) in water-in-oil (w/o) emulsion were measured in a flat-stirred vessel at 25°C. The effects of reactant concentration, size of aqueous droplets, volume fraction of continuous phase, and stirring speed on the absorption rate of CO_2 were investigated. The absorption mechanism of CO_2 into the continuous benzene phase through a gas–liquid interface was described on the basis of the penetration model, while the subsequent absorption/reaction in the dispersed aqueous droplets was modeled by the film model.

Key Words: Gas absorption; Carbon dioxide; Emulsion; Amine

*Corresponding author. E-mail: swpark0@hyowon.pusan.ac.kr

INTRODUCTION

Nowadays the global warming issue caused by greenhouse gases has become a matter of great concern, and carbon dioxide, which is produced in enormous amounts, has been recognized widely as one of the most influential greenhouse gases. Many sites such as fossil–fuel-fired power plants, iron and steel works, and cement works discharge a huge amount of CO_2 day after day. The fixation and removal of CO_2 from fossil–fuel combustion facilities has been considered as a way to prevent atmospheric CO_2 buildup. The chemical absorption and membrane based on the separation processes are the possible promising process by which CO_2 can be reduced successfully from industrial waste gases and other gaseous mixtures.

Artificial membranes have been a topic of great interest in recent years because of their potential applications. One of the most intriguing classes of artificial membranes is the liquid membrane. In general, there are two main types of liquid membrane systems that have been considered for practical applications, i.e., emulsion-type liquid membrane and supported liquid membrane. Emulsion-type liquid membrane is made by forming emulsions of two immiscible phases and then dispersing them in a third phase (the continuous phase). The emulsion is stabilized by surfactants. The liquid-membrane processes have been investigated for the separation of metals (1–3) and hydrocarbons (3–6).

It is known that the dispersed second liquid in water-in-oil (w/o) emulsion can enhance the mass transfer of a dissolved gas in a gas–liquid system. A qualitative explanation of this phenomenon has been given by various authors: small droplets of a liquid immiscible with the continuous liquid phase absorb the gas in the hydrodynamic mass-transfer film, after which desorption of the gas takes place in the gas-poor bulk of the liquid.

Linek and Benes (7) have studied gas absorption into oil-in-water (o/w) emulsion or w/o emulsion. In o/w type emulsions, the mass transfer coefficient is not affected by the content of the oil phase, whereas in the w/o type emulsion, the coefficient increases in proportion to the volume fraction of oil.

Mehra and Sharma (8,9) have reported a study on the absorption of isobutylene, butene-1, and propylene in microemulsions of chlorobenzene in aqueous solutions of sulfuric acid, where enhancement factors as high as 25 have been achieved. They have suggested that the specific rate of absorption of a sparingly soluble gas, in a liquid where reaction occurs, may be substantially enhanced by the use of a second liquid phase, which is immiscible with the original liquid phase but exhibits a pronounced solubility for the gas. The second liquid phase may be simply dispersed or emulsified. The emulsion may have dispersed-liquid droplets in size smaller than the diffusional film thickness.

Enhancements of rates are expected due to an additional mode of transport of the solute gas via the second liquid phase.

Bruining et al. (10) have studied the absorption of oxygen into o/w emulsions. It has been shown that the rate of mass transfer of oxygen into an aqueous sulfite solution can be enhanced by the presence of small amounts of a dispersed organic phase. Mehra (11) and Mehra et al. (12) have analyzed the process of absorption of gases into emulsion of an additional liquid phase on the basis of the unsteady-state theory and compared the predicted enhancement factors with the measured ones.

As mentioned above, the dispersed phase plays the role of a carrier that transports the dissolved gas from the gas–liquid interface to the bulk body of the liquid and the reaction of the dissolved gas with reactant occurs in the continuous phase.

If the system is w/o type emulsion such that the dispersed phase is the aqueous-solution containing reactant, and the continuous phase is the organic solvent having larger solubility of gas than water, then the specific rate of absorption may be enhanced because of larger solubility and chemical reaction.

In this study, the absorption mechanism of CO_2 into w/o emulsion composed of aqueous amine solution and benzene is presented, and the measured absorption rates of CO_2 are compared with those obtained from the model based on the penetration theory with chemical reaction. Monoethanolamine (MEA), diethanolamine (DEA), and triethanolamine (TEA) were used as reagents of CO_2.

THEORY

In case of absorption of CO_2 into w/o emulsion with benzene–aqueous amine solution as shown in Fig. 1, the mathematical model is developed to describe the absorption of CO_2 into the continuous benzene phase through the gas–liquid interface under unsteady-state and transfer into the dispersed aqueous droplets through the liquid–liquid interface under steady-state, where the chemical reaction of CO_2 occurs.

The following assumptions are made to set up the conservation equations: (1) Henry's law holds, (2) the reaction of CO_2 with reactant occurs in the aqueous droplets and is first-order with respect to both CO_2 and reactant, (3) isothermal condition prevails, (4) size and shape of the dispersed aqueous droplets are uniform and sphere, and (5) although the solubilities (13) of MEA, DEA, and TEA in benzene at 25°C are 1.4, 4.2, and 4.2% respectively, these solubilities in benzene are assumed to be zero.

Under these assumptions, the conservation equations of CO_2 absorbed in the dispersed aqueous phase are given as

$$D_{eA}\left(\frac{d^2 c_A}{d r^2}+\frac{2d c_A}{r d r}\right)=k_2 c_A c_B \tag{1}$$

$$D_{eB}\left(\frac{d^2 c_B}{d r^2}+\frac{2d c_B}{r d r}\right)=\nu k_2 c_A c_B \tag{2}$$

Boundary conditions to be imposed are

$$r=R; \qquad c_A=c_A^*=H_A C_A, \qquad \frac{d c_B}{d r}=0 \tag{3}$$

$$r=0; \qquad \frac{d c_A}{d r}=\frac{d c_B}{d r}=0 \tag{4}$$

Eqs. (1) and (2) and the boundary conditions are put into dimensionless forms as follows:

$$\frac{d^2 \alpha_A}{d y^2}+\frac{2d \alpha_A}{y d y}=m_A^2 \alpha_A \alpha_B \tag{5}$$

$$\frac{d^2 \alpha_B}{d y^2}+\frac{2d \alpha_B}{y d y}=\frac{m_A^2}{r_B q_B}\alpha_A \alpha_B \tag{6}$$

$$y=1; \qquad \alpha_A=1, \qquad \frac{d \alpha_B}{d y}=0 \tag{7}$$

$$y=0; \qquad \frac{d \alpha_A}{d y}=\frac{d \alpha_B}{d y}=0 \tag{8}$$

where $\alpha_A=c_A/c_A^*$, $\alpha_B=c_B/c_{B0}$, $y=r/R$, $m_A=R\sqrt{k_2 c_{B0}/D_{eA}}$, $r_B=D_{eB}/D_{eA}$, $q_B=c_{B0}/\nu c_A^*=q_{B0}/Y_A$, $q_{Bo}=c_{Bo}/\nu H_A C_{Ai}$, and $Y_A=C_A/C_{Ai}$.

The effectiveness factor here can be defined as

$$E_f=\frac{4\pi R^2 n_A}{(4/3)\pi R^3 k_2 c_A^* c_{B0}}=\left.\frac{3d \alpha_A}{m_A^2 d y}\right|_{y=1} \tag{9}$$

where n_A is the flux of CO_2 defined as $D_{eA} d c_A/d r|_{r=R}$.

MARCEL DEKKER, INC.
270 Madison Avenue, New York, New York 10016

The conservation equation for the dissolved gas in the continuous liquid phase at unsteady-state can be written as

$$D_A \frac{\partial^2 C_A}{\partial z^2} = \frac{\partial C_A}{\partial t} + (1 - \varepsilon) k_2 c_{B0} H_A C_A E_f \tag{10}$$

Boundary and initial conditions are given as

$$z = 0, \qquad t > 0; \qquad C_A = C_{Ai} \tag{11}$$

$$z > 0, \qquad t = 0; \qquad C_A = 0 \tag{12}$$

$$z = \infty, \qquad t > 0; \qquad C_A = 0 \tag{13}$$

Eqs. (10)–(13) are put into the dimensionless form as follows:

$$\frac{\partial^2 Y_A}{\partial x^2} = \frac{\partial Y_A}{\partial \theta} + E_f Y_A \tag{14}$$

$$x = 0, \qquad \theta > 0; \qquad Y_A = 1 \tag{15}$$

$$x > 0, \qquad \theta = 0; \qquad Y_A = 0 \tag{16}$$

$$x = \infty, \qquad \theta > 0; \qquad Y_A = 0 \tag{17}$$

where, $Y_A = C_A/C_{Ai}$, $\theta = (1 - \varepsilon) k_2 c_{Bo} H_A t$, $x = z\sqrt{(1 - \varepsilon) k_2 c_{Bo} H_A D_A}$ and $M = (1 - \varepsilon) k_2 c_{B0} H_A D_A / k_L^2$.

The molar flux of CO_2 with chemical reaction at any contact time θ is defined as

$$N_A = -D_A \left. \frac{\partial C_A}{\partial z} \right|_{z=0} \tag{18}$$

The mean molar flux of CO_2 during contact time, t, is written as

$$\bar{N}_A = \frac{1}{t} \int_0^t N_A \, dt \tag{19}$$

MARCEL DEKKER, INC.
270 Madison Avenue, New York, New York 10016

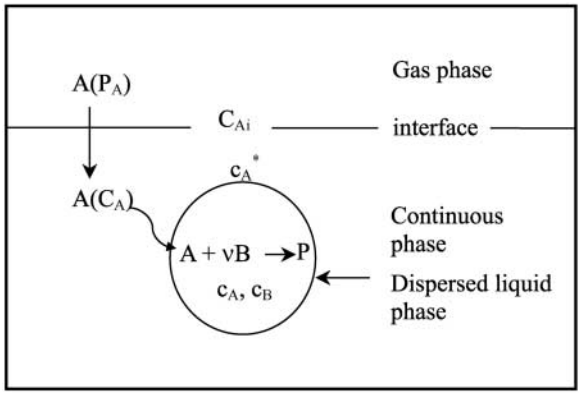

Figure 1. Chemical absorption path of gas (A) into w/o emulsion.

The mean molar flux without chemical reaction based on the penetration model during contact time has been derived as follows (14):

$$\bar{N}_{\mathrm{A}}^{0} = 2C_{\mathrm{Ai}}\sqrt{\frac{D_{\mathrm{A}}}{\pi t}} \tag{20}$$

The enhancement factor (ϕ) here defined as the ratio of molar flux with chemical reaction to that without chemical reaction, is described by using Eqs. (19) and (20) as follows:

$$\phi = \frac{\bar{N}_{\mathrm{A}}}{\bar{N}_{\mathrm{A}}^{0}} = -\frac{\sqrt{M}}{t}\int_{0}^{t}\left.\frac{\partial Y_{\mathrm{A}}}{\partial x}\right|_{x=0} \mathrm{d}\,t \tag{21}$$

EXPERIMENTAL

All chemicals in this study were reagent grade, and used without further purification. Purity of both CO_2 and N_2 gases was more than 99.9%. The w/o type emulsion from benzene and aqueous amine solution was made by the same procedure as those reported elsewhere (15) by adding Tween 80 (Aldrich Chem. Co.) and Arlacel 83 (Aldrich Chem. Co.) as surfactant, by using a homogenizer (Fisher Scientific Co.) in the range of agitation speed of 1500–10,000 rev/min, and the mean size of aqueous droplets was measured by Image Analyzer (Leitz TAS Plus Co.). The absorption rates of CO_2 with a flat stirred vessel were

measured along the procedure identical to those reported elsewhere (16) at 25°C and an atmospheric pressure. For the absorption experiments, the range of concentration of reactant was 0.5–2.0 kmol/m^3, that of agitation speed, 100–200 rev/min, that of droplet radius, $2-15\times10^{-6}$ m and that of volume fraction of continuous phase, 0.6–0.8.

Absorption experiments were carried out in a magnetic stirred absorber with a flat gas–liquid interface. The vessel was of 10.2 cm inside diameter and of 15.1 cm in height, and was of similar design to that used in the previous work (16). The vessel was constructed of glass. Four equally spaced vertical baffles, each one-tenth of the vessel diameter in width, were attached to the internal wall of the vessel. The liquid phase was agitated with a magnetic stirrer without agitation in the gas phase because of pure CO_2 gas. The absorption rate of CO_2 was obtained according to the same experimental procedure reported elsewhere (16). A sketch of the experimental set-up is presented in Fig. 2. A typical experimental run was carried out as follows.

The vent-valve A is initially closed and the purge-valve B is open. CO_2 is flowed continuously through the absorber C, so as to make sure that the latter is filled with CO_2 at the start of the experiment. During this initial period, the water-bath temperature is brought up to the desired value, and the liquid batch is kept in bottle D inside the water bath.

At the start of the experiment, the liquid batch is poured into funnel E and the stirrer in C is started. The liquid feed-valve F is opened, the purge-valve B is closed, and the vent-valve A is opened, as simultaneously as possible. Measurements are started at the soap-film meter G taking care that there are always two soap films in the meter so that a continuous reading of the cumulative

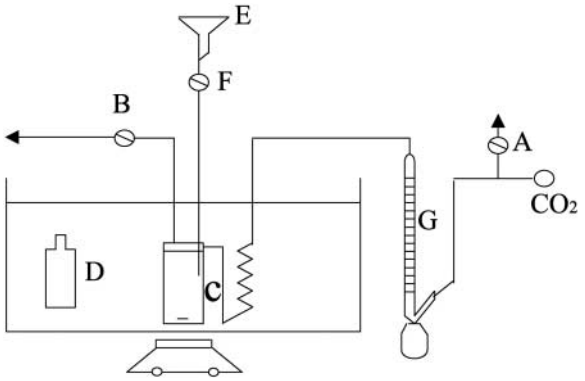

Figure 2. Sketch of the experimental set-up.

volume of CO_2 which has flowed through the meter, $V(t)$, can be recorded as a function of time.

The instantaneous molar-absorption rate, R_A, was calculated as:

$$R_A = \frac{V(t_2) - V(t_1)}{(t_2 - t_1)v} \tag{22}$$

where t_1 and t_2 are successive times for which values of V were recorded, and v is the molar volume of CO_2 at the conditions prevailing in the soap film meter. Values of R_A from Eq. (22) were constant, within experimental accuracy, over a few consecutive time periods, and were taken as a mean value with three repeated experimental runs.

PHYSICOCHEMICAL PROPERTIES

In the reaction of CO_2 with MEA (17), DEA (18), and TEA (19), the reaction rate constants were estimated as follows:

For MEA, $\log k_2 = 10.99 - (2152/T)$
For DEA, $\log k_2 = 10.4493 - (2274.5/T)$
For TEA, $\log k_2 = 6.934 - (1898.2/T)$

The value of diffusivity of CO_2 in benzene estimated from the Wilke–Chang Eq. (20) was $3.853\times10^{-9}\,m^2/s$ at 25°C.

The values of diffusivity of CO_2 in MEA, DEA, and TEA (21) solutions were estimated as follows:

For MEA, $D_{eA} = (1.9686 - 0.1843c_{B0} - 0.0429c_{B0}^2)\times 10^{-9}$
For DEA, $D_{eA} = (1.9686 - 0.8103c_{B0} - 0.1771c_{B0}^2)\times 10^{-9}$
For TEA, $D_{eA} = (1.978 - 0.57c_{B0} - 0.02c_{B0}^2)\times 10^{-9}$

The ratio of diffusivity of reactant to that of CO_2 in benzene(r_B) was assumed to be equal to the ratio in water, i.e., $D_{eB}/D_{eA} = D_{eBW}/D_{eAW}$ (22). The diffusivities of MEA, DEA, and TEA (21) in water at 25°C have been reported to be $1.1\times10^{-9}\,m^2/s$, $6.67\times10^{-10}\,m^2/s$, and $7.11\times10^{-10}\,m^2/s$, respectively.

The values of solubility of CO_2 in benzene and water were $0.1107\,kmol/m^3$ (15) and $0.035\,kmol/m^3$ (20) at 25°C and 0.101 MPa, respectively. The values of solubility of CO_2 in MEA (17), DEA (18), and TEA (23) solutions were estimated as follows:

For MEA,

$$\log\left(\frac{c_A^*}{c_{Aw}^*}\right) = \frac{0.3c_{B0}}{1 + 0.963c_{B0}}$$

MARCEL DEKKER, INC.
270 Madison Avenue, New York, New York 10016

For DEA,

$$\log\left(\frac{c_A^*}{c_{Aw}^*}\right) = -(1.0406\times10^{-4} + 6.8433\times10^{-6}c_{B0} + 1.33633\times10^{-8}c_{B0}^2 - 1.1549\times10^{-12}c_{B0}^3)$$

For TEA,

$$c_A^* = 2.1\times10^{-7}\exp\left(\frac{1572.2}{T}\right)$$

The distribution coefficient of CO_2 between benzene and aqueous solution, H_A, was obtained from the ratio of the solubility of CO_2 in benzene to that in aqueous solution.

The mass transfer coefficient, k_L, of CO_2 in CO_2/emulsion system without reactant in the aqueous droplets was measured along the procedure as reported elsewhere (15) and the values at agitation speeds of 100, 150, and 200 rev/min were 4.55×10^{-5}, 5.13×10^{-5}, and 10.34×10^{-5} m/s, respectively.

The stoichiometric coefficients, ν, in Eq. (2) for MEA, DEA, and TEA were obtained from the reference, and their values were 2 (17), 2 (18), and 1 (19), respectively.

RESULTS AND DISCUSSION

The concentration of A in the droplets, α_A, is obtained from the numerical solution of Eqs. (5) and (6) with the boundary conditions, Eqs. (7) and (8), and then the value of E_f is obtained from Eq. (9). If the concentration of B in the droplets, c_B is constant, the value of E_f can be obtained from the exact solution of Eqs. (5) and (6).

If c_B is equal to the feed concentration, c_{Bo}, the differential equation of Eq. (5) and the boundary conditions of Eqs. (7) and (8) are reduced to

$$\frac{d^2\alpha_A}{dy^2} + \frac{2\,d\alpha_A}{y\,dy} = m_A^2\alpha_A \tag{23}$$

$$y = 1; \qquad \alpha_A = 1 \tag{24}$$

$$y = 0; \qquad \frac{d\alpha_A}{dy} = 0 \tag{25}$$

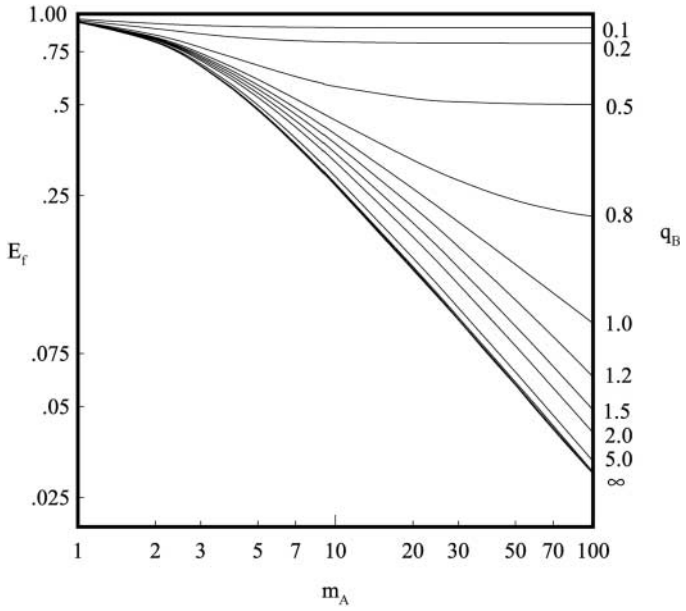

Figure 3. Effect of m_A on effectiveness factor for various values of q_B.

The concentration profile of A derived from the exact solution of Eq. (23) is given as follows:

$$\alpha_A = \frac{\sinh(m_A y)}{y \sinh(m_A)} \tag{26}$$

And using Eqs. (9) and (26), E_f is derived as

$$E_f = \frac{3}{m_A}\left(\frac{1}{\tanh(m_A)} - \frac{1}{m_A}\right) \tag{27}$$

If c_B is equal to the interfacial constant concentration between the continuous and dispersed phase, c_{Bi}, α_A is derived from the exact solution of Eq. (5) as follows:

$$\alpha_A = \frac{\sinh(m_A \eta y)}{y \sinh(m_A \eta)} \tag{28}$$

where, $\eta = \sqrt{\alpha_{Bi}} = \sqrt{c_{Bi}/c_{Bo}}$

MARCEL DEKKER, INC.
270 Madison Avenue, New York, New York 10016

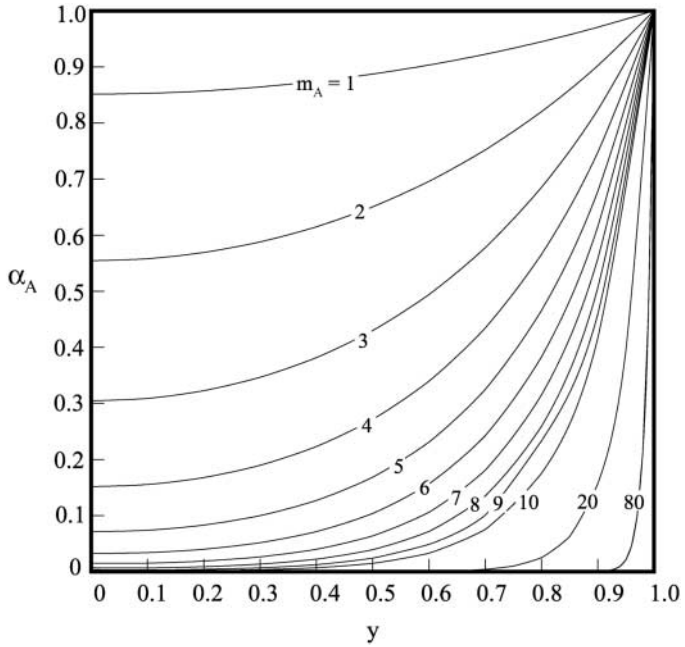

Figure 4. Dimensionless concentration profiles of CO_2 in the dispersed phase for various values of m_A at $M = 40$ and $q_B^0 = 20$.

Using Eqs. (9) and (28), E_f is derived as

$$E_f = \frac{3}{m_A \eta}\left[\frac{1}{\tanh(m_A \eta)} - \frac{1}{m_A \eta}\right] \tag{29}$$

The mass balance between the component A and B in the droplets is written as follows:

$$\frac{4}{3}\pi R^3 (c_{Bo} - c_{Bi}) = \nu \int_0^R 4\pi r^2 (c_A^* - c_A) \mathrm{d}\, r \tag{30}$$

The Eq. (30) is put into dimensionless form as follows:

$$1 - \alpha_{Bi} = \frac{3}{q_B}\int_0^1 y^2 (1 - \alpha_A) \mathrm{d}\, y \tag{31}$$

MARCEL DEKKER, INC.
270 Madison Avenue, New York, New York 10016

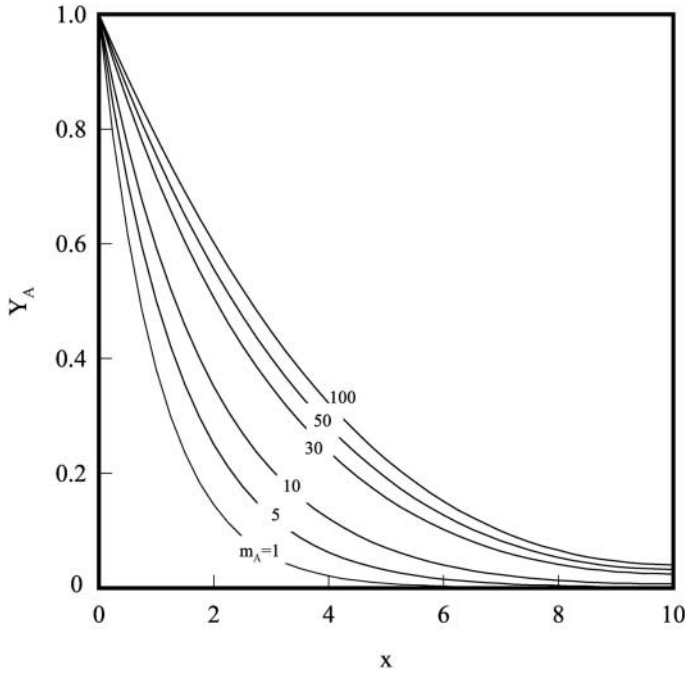

Figure 5. Concentration profile of CO_2 in the continuous phase at various values of m_A at $M = 40$.

α_{Bi} is derived from Eq. (31) with Eq. (9) and (28) as follows:

$$\alpha_{Bi} = 1 - \frac{1 - E_f}{q_B} \tag{32}$$

In order to observe the effect of m_A on E_f at $c_B = c_{Bi}$, the values of E_f calculated from Eq. (29) were plotted for various values of m_A with a parameter of q_B in Fig. 3. As shown in Fig. 3, E_f decreased with increasing m_A for a parameter of q_B. This means that the reaction rate between A and B in the droplets is larger than the mass-transfer rate of A from the continuous phase to the dispersed one. In addition, E_f decreased with increasing q_B for a parameter of m_A, and approached to an asymptote. This means that α_{Bi} is close to 1 from Eq. (32) for very large values of q_B, i.e., $q_B = \infty$, and α_A from Eq. (28) approach to that from Eq. (26). If the reaction rate is very fast and its feed concentration of B, c_{Bo} is larger than c_A^*, c_B becomes constant c_{Bo}, and this reaction regime becomes a pseudo-first-order fast reaction regime.

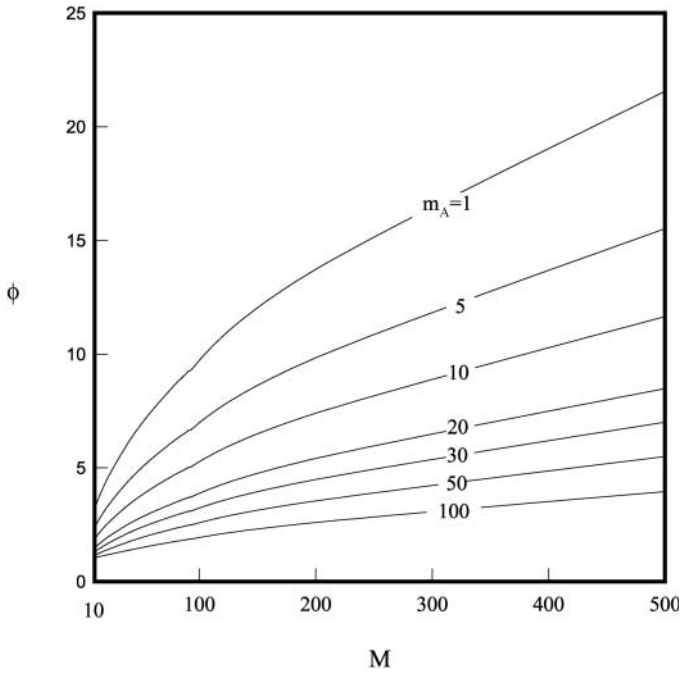

Figure 6. Effect of M on ϕ for various values of m_A.

Table 1. Classification of Reaction Regime

Amine	c_{Bo} (kmol/m^3)	$\sqrt{D_{EA}k_2c_{Bo}}/k_L$	$c_{Bo}\sqrt{D_{EB}/D_{EA}}/c_A^*$
MEA	0.5	22.63	4.23
	1.0	30.92	7.51
	1.5	36.25	10.48
	2.0	39.60	13.32
DEA	0.5	4.16	7.07
	1.0	8.32	9.12
	1.5	10.38	12.07
	2.0	11.49	16.63
TEA	0.5	0.54	7.31
	1.0	0.69	14.63
	1.5	0.75	21.94
	2.0	0.72	29.26

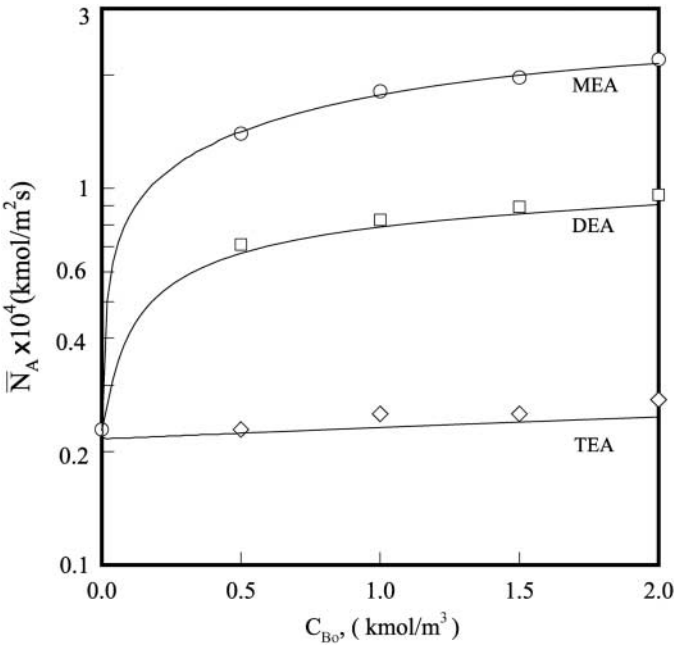

Figure 7. Effect of amine concentration on the mean molar flux for various amines at $R = 10\,\mu\text{m}$, $k_L = 1.034 \times 10^{-4}\,\text{m/s}$, and $\varepsilon = 0.6$.

In order to observe the effects of m_A on the concentration profile of CO_2 in the aqueous droplets in the case of the pseudo-first-order fast reaction regime, the concentration of CO_2 can be calculated from Eq. (26). Figure 4 shows the typical concentration profiles of CO_2 with a parameter of m_A for M of 40 and q_{Bo} of 20. As shown in Fig. 4, α_A increases as y approaches 1. The slope of plots at the surface of the aqueous droplet, $d\,\alpha_A/d\,y$ at $y = 1$, increases with increasing m_A, from which E_f will increase. From comparison of this result with the decreasing trend in Fig. 3, it may be said that m_A influences E_f more than the slope does.

In order to observe the effects of m_A and M on the concentration profile of CO_2 in the continuous phase in the case of the pseudo-first-order fast reaction regime, Y_A was obtained from the numerical solution to Eq. (14) by the finite difference method with centered difference formula for variable x and forward difference formula for variable θ.

Figure 5 shows typical plots of Y_A against x at various values of m_A at θ of 10. As shown in this figure, Y_A decreased as the depth from the gas–liquid interface increased and m_A decreased.

As shown in Eq. (21), the enhancement factor, ϕ is a function of M and m_A. In order to observe the effects of m_A and M on the enhancement factor in the case of the pseudo-first-order fast reaction regime, was calculated using Eq. (21). Figure 6 shows a plot of ϕ against M with m_A as a parameter. As shown in Fig. 6, ϕ increased with increasing M and decreasing m_A. Because the slope of the plots at the gas–liquid interface, dY_A/dx at $x = 0$, increases with decreasing m_A as shown in Fig.5, ϕ increases with decreasing m_A from Eq. (21).

In order to ascertain the effect of chemical reaction on the specific rate of mass transfer, the system in this study may be classified into slow reaction regime and fast one depending on the relative rate of diffusion and chemical reaction (24). The values of $\sqrt{D_{eA}k_2c_{Bo}}/k_L$, and $c_{Bo}\sqrt{D_{eB}/D_{eA}}/c_A^*$ for MEA, DEA, and TEA were calculated using the physicochemcal properties such as D_{eA}, D_{eB}, k_2, c_A^* in range of the reactant concentration of 0.5–2.0 kmol/m^3, and k_L measured at the agitation speed of 200 rev/min, and were listed in Table 1. As shown in Table 1, $\sqrt{D_{eA}k_2c_{Bo}}/k_L$ is larger than $c_{Bo}\sqrt{D_{eB}/D_{eA}}/c_A^*$ for MEA, the former is smaller than the latter for DEA, and the former is smaller than 1 for TEA. Therefore, the

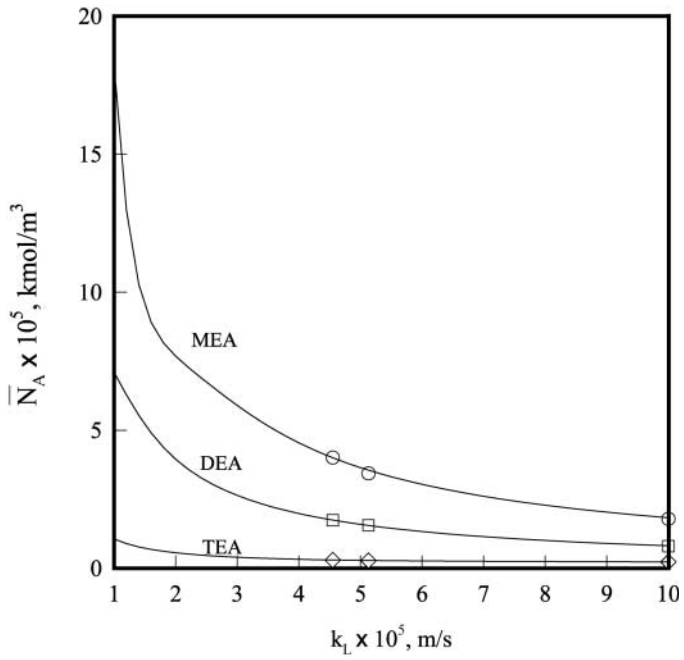

Figure 8. Effect of mass transfer coefficient on the mean molar flux for various amines at $c_{Bo} = 1.0\,\text{kmol/m}^3$, $R = 10\,\mu\text{m}$, and $\varepsilon = 0.6$.

system of the chemical reaction of CO_2 with MEA is the instantaneous reaction regime, the system with DEA is the fast reaction regime, but the system with TEA is the slow reaction regime.

The absorption rate of CO_2 was measured according to change of reactant concentration of 0.5, 1.0, 1.5, and 2.0 kmol/m^3 for the various species of amine under the typical experimental conditions such as agitation speed of 200 rev/min, aqueous droplet size of 10 μm in emulsion prepared at 5000 rev/min, and volume fraction of 0.6, in order to observe the effect of c_{Bo} on $\bar{N}_A$.

Figure 7 shows a plot of the mean molar flux of CO_2 against the concentration of reactant for various species of amines. The solid curves represent the calculated values from Eq. (19) at the contact time of 0.1148 s, which was calculated as $D_A/\pi k_L^2$ from comparison of the penetration theory with the film theory, and the symbols refer to experimental data. E_f in the partial differential equation of Eq. (14) is obtained from Eq. (26) for MEA and DEA. E_f for TEA is obtained from solution of simultaneous differential equation of Eqs. (5) and (6) with boundary conditions of Eqs. (7) and (8), because of the slow reaction regime of TEA.

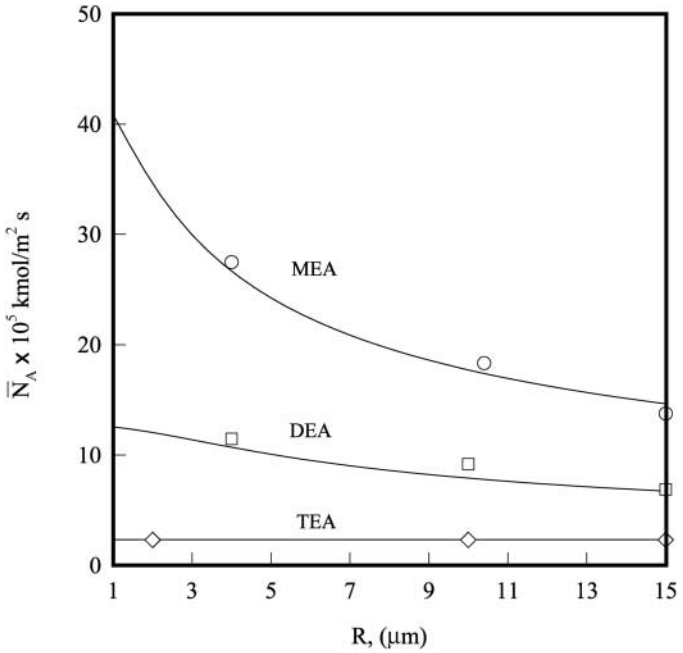

Figure 9. Effect of liquid droplet size on the mean molar flux for various amines at $c_{Bo} = 1.0\,\text{kmol/m}^3$, $k_L = 1.034 \times 10^{-4}\,\text{m/s}$, and $\varepsilon = 0.6$.

MARCEL DEKKER, INC.
270 Madison Avenue, New York, New York 10016

The measure and calculated values of N_A^0 in Fig. 7 were 2.08 and 2.30 kmol/m^3 s, respectively. As shown in Fig. 7, the experimental values approach reasonably to the calculated ones, and $\bar{N}_A$ increases with increasing reactant concentration. In this figure, $\bar{N}_A$ also depends on the species of reactant. In other words, it increases in the order of MEA, DEA, and TEA. This is caused by the fact that the reaction rate constant for the reactant increases in the order of the reactants, i.e., the reaction rate constants of MEA, DEA, and TEA are 5868, 656, and 3.7 m^3/kmol s, respectively.

The measured and calculated values of $\bar{N}_A$ for TEA were very low and were close to $\bar{N}_A^0$. This is explained by the fact that the chemical reaction of CO_2 with the tertiary amine such as TEA probably does not occur since no proton transfer can be involved in the reaction scheme (19).

Figure 8 shows a plot of the mean molar flux of CO_2 against mass transfer coefficient, which depends on the agitation speed, under the typical experimental conditions such as reactant concentration of 1.0 kmol/m^3, droplet size of 10 μm, and volume fraction of 0.6. As shown in Fig. 8, the solid curves represent the calculated values from Eq. (19) using the same procedure mentioned in Fig. 7. $\bar{N}_A$

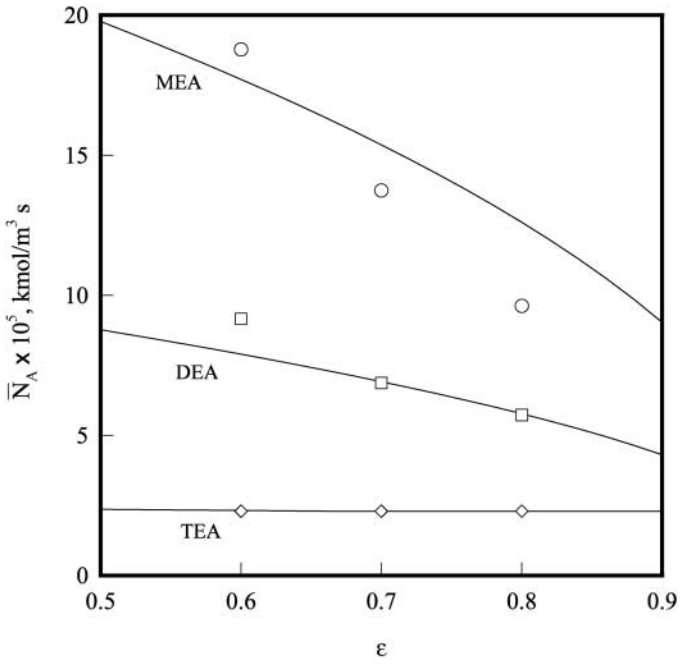

Figure 10. Effect of volume fraction of continuous phase on the mean molar flux for various amines at $c_{Bo} = 1.0\,\text{kmol/m}^3$, $R = 10\,\mu\text{m}$, and $k_L = 1.034 \times 10^{-4}\,\text{m/s}$.

was decreased with increasing mass transfer coefficient, i.e., increasing of agitation speed. This tendency can be explained by the fact that M decreases with increasing mass transfer coefficient.

The aqueous droplet size in the w/o emulsion was adjusted by the agitation speed of the homogenizer. The mean sizes of the droplet for MEA and DEA at the agitation speed of 1500, 5000, and 10,000 rev/min were 4, 10, and 15 μm, respectively, and those for TEA, 2, 10, and 15 μm, respectively. The absorption rate of CO_2 was measured in the same volume of emulsion made according to change of the agitation speed in order to observe the effect of the droplet size on $\bar{N}_A$. Figure 9 shows a typical plot of the mean molar flux of CO_2 against droplet size at reactant concentration of 1.0 kmol/m^3, agitation speed of 200 rev/min and volume fraction of 0.6. The solid curves represent the calculated values from Eq. (19) using the same procedure mentioned in Fig. 7. As shown in Fig. 9, $\bar{N}_A$ decreases with increasing droplet size. This may be explained by the fact that m_A increases with increasing droplet size, and the ratio of the interfacial area between benzene and aqueous phase to the volume of aqueous phase decreases with increasing droplet size.

The absorption rate of CO_2 was measured according to change of benzene volume fraction of 0.6, 0.7, and 0.8 in order to observe the effect of ϵ on $\bar{N}_A$. Figure 10 shows a typical plot of the mean molar flux of CO_2 against volume fraction of benzene at reactant concentration of 1.0 kmol/m^3, agitation speed of 200 rev/min, and droplet size of 10 μm. The solid curves represent the calculated values from Eq. (19) using the same procedure mentioned in Fig. 7. As shown in Fig. 10, $\bar{N}_A$ decreased with increasing volume fraction of benzene. This is explained by the fact that M decreases with increasing ϵ and the total volume of the aqueous phase becomes small and the reaction zone becomes narrow with an increase of the volume of benzene phase.

It is necessary to generalize the relationship between the mean molar flux of CO_2 and the experimental variables presented in Figs. 6–9, because the enhancement factor was effected on M and m_A, respectively, as shown in Fig. 5. Figure 11 shows a plot of the enhancement factor against the product of E_f and M for the pseudo-first-order reaction regime. The solid curves represent the calculated values from Eq. (21) and the symbols refer to the experimental data for MEA and DEA. As shown in this figure, the experimental values of ϕ approached reasonably to the calculated ones, and ϕ increased with an increase of the product of E_f and M, from which ϕ could be expressed as a function of the product of E_f and M.

CONCLUSION

Carbon dioxide was absorbed into w/o emulsion composed of aqueous amine solution such as MEA, DEA and TEA, and benzene using a stirred vessel

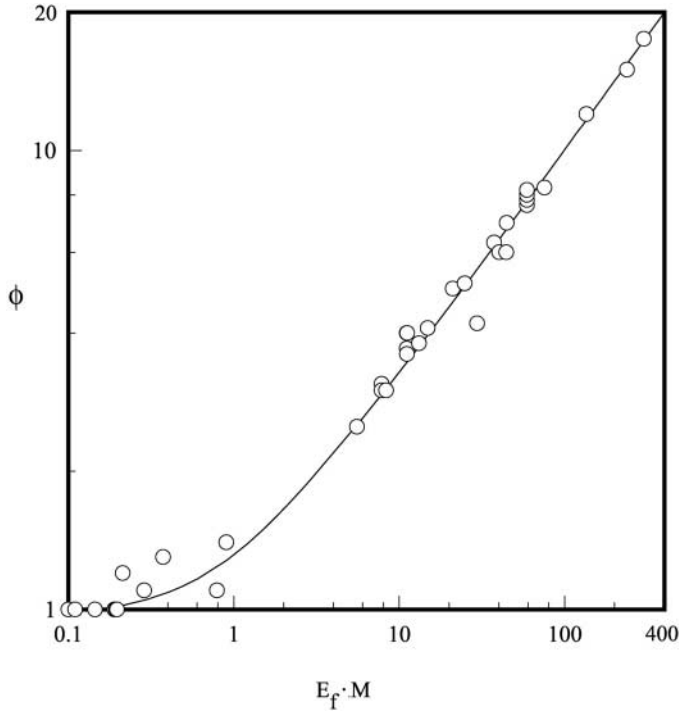

Figure 11. Effect of the multiplication of E_f and M on enhancement factor.

with a flat gas–liquid interface at 25°C and an atmospheric pressure. The measured rate of CO_2 absorption increased with increasing reactant concentration, whereas it decreased with increasing agitation speed, size of aqueous droplet, and volume fraction of benzene.

A mathematical model was developed as a combination of physical absorption into the continuous phase through the gas–liquid interface on the basis of the penetration model and chemical absorption into the dispersed phase through the liquid–liquid interface on the basis of film model.

The reaction regime of the CO_2/amine system with w/o emulsion was classified into three kinds of reaction regime such as the instantaneous reaction regime for MEA, the fast one for DEA, and the slow one for TEA with the physicochemical properties of the system. The mean molar flux of CO_2 calculated by the numerical analysis of the proposed model of diffusion with chemical reaction approached reasonably to the experimental values.

NOMENCLATURE

C_A	concentration of CO_2 in benzene (kmol/m^3)
c_A	concentration of CO_2 in aqueous phase (kmol/m^3)
c_A^*	solubility of CO_2 in aqueous phase (kmol/m^3)
C_{Ai}	solubility of CO_2 in water (kmol/m^3)
c_{Aw}^*	feed concentration of CO_2 in water (kmol/m^3)
c_B	concentration of amine in aqueous phase (kmol/m^3)
c_{Bo}	solubility of CO_2 in benzene (kmol/m^3)
D_A	diffusivity of CO_2 in benzene (m^2/s)
D_{ei}	diffusivity of component i in aqueous phase (m^2/s)
E_f	effectiveness factor defined as by Eq. (9)
H_A	dimensionless solubility defined as c_A^*/C_A
k_2	2nd order reaction rate constant (m^3/kmol s)
k_L	mass transfer coefficient of CO_2 in benzene (m/s)
M	dimensionless modulus defined as $(1-\varepsilon)k_2 c_{B0} H_A D_A / k_L^2$
m_A	dimensionless modulus defined as $R\sqrt{k_2 c_{B0}/D_{eA}}$
N_A	molar flux of CO_2 at gas–liquid interface with chemical reaction in benzene at constant time (kmol/m^2 s)
$\bar{N}_A$	mean molar flux of CO_2 at gas–liquid interface with chemical reaction in benzene during contact time (kmol/m^2 s)
N_A^0	molar flux of CO_2 at gas–liquid interface without chemical reaction in benzene at constant time (kmol/m^2 s)
$\bar{N}_A^0$	mean molar flux of CO_2 at gas–liquid interface without chemical reaction in benzene during contact time (kmol/m^2 s)
n_A	mass transfer rate of CO_2 from benzene phase into aqueous phase (kmol/m^2 s)
r	radial distance in aqueous phase (m)
R	radius of aqueous droplet in benzene phase
R_A	instantaneous molar absorption rate of CO_2 (kmol/s)
r_B	diffusivity ratio defined as D_{eB}/D_{eA}
q_B	dimensionless concentration defined as c_{B0}/c_A^*
q_B^o	dimensionless concentration defined as $c_{B0}/\nu H_A C_{Ai}$
t	time (s)
T	temperature (K)
v	molar volume of CO_2 at 25°C and 1 atm (m^3/kmol)
V	cumulative volume of CO_2 at 25°C and 1 atm (m^3)
x	dimensionless coordinate in film thickness direction in benzene phase defined as $z\sqrt{(1-\varepsilon)k_2 c_{B0} H_A / D_A}$

MARCEL DEKKER, INC.
270 Madison Avenue, New York, New York 10016

Y_A dimensionless concentration in benzene phase
y dimensionless radial coordinate defined as r/R
z coordinate in film thickness direction in benzene phase (m)

Greek Letters

α_A dimensionless concentration of CO_2 component in aqueous phase defined as c_A/c_{A0}
α_B dimensionless concentration of B component in aqueous phase defined as c_B/c_{B0}
ϵ volume fraction of benzene phase in the emulsion
θ dimensionless time defined as $(1-\epsilon)k_2c_{Bo}H_At$
$\emptyset$ enhancement factor
ν stoichiometric coefficient in chemical reaction of CO_2 with amine

Subscripts

A CO_2
B reactant (amine)
E aqueous
I gas–liquid interface
o bulk body
W pure water phase
* liquid–liquid interface

ACKNOWLEDGMENTS

This work was supported by grant No. (2000-2-30700-002-3) from the Basic Research Program of the Korea Science and Engineering Foundation.

REFERENCES

1. Chan, C.C.; Lee, C.J. Mechanistic Models of Mass Transfer Across a Liquid Membrane. J. Membr. Sci. **1984**, *20*, 1–24.
2. Bunge, A.L.; Noble, R.D.J. A Diffusion Model for Reversible Consumption in Emulsion Liquid Membranes. J. Membr. Sci. **1984**, *21*, 55–71.
3. Bunge, A.L.; Noble, R.D. Batch Extraction of Amines Using Emulsion Liquid Membranes. Importance of Reaction Reversibility. AIChE. J. **1987**, *33* (1), 43–54.
4. Teramoto, M.; Takihara, H.; Shibutnani, M.; Yuasa, T.; Miyake, Y.; Teranishi, T. Extraction of Amine by w/o/w Emulsion System. J. Chem. Eng. Jpn. **1981**, *14* (2), 122–128.

MARCEL DEKKER, INC.
270 Madison Avenue, New York, New York 10016

5. Ho, W.S.; Hatton, T.A.; Lightfoot, E.N.; Li, N.N. Batch Extraction with Liquid Surfactant Membranes: A Diffusion Controlled Model. AIChE. J. **1982**, *28* (4), 662–670.
6. Kim, K.S.; Choi, S.J.; Ihm, S.K. Simulation of Phenol Removal from Waste Water by Liquid Membrane Emulsion. Ind. Eng. Chem. Fundam. **1983**, *22*, 167–172.
7. Linek, V.; Benes, P. A Study of the Mechanism of Gas Absorption into Oil–Water Emulsions. Chem. Eng. Sci. **1976**, *31*, 1037–1046.
8. Mehra, A.; Sharma, M.M. Absorption with Reaction: Effect of Emulsified Second Liquid Phase. Chem. Eng. Sci. **1985**, *40* (12), 2382–2385.
9. Mehra, A.; Sharma, M.M. Absorption with Reaction in Microemulsions Absorption of Olefins. Chem. Eng. Sci. **1986**, *41* (9), 2455–2456.
10. Bruining, W.J.; Joosten, G.E.H.; Beenackers, A.A.C.M.; Hofman, H. Enhancement of Gas–Liquid Mass Transfer by a Dispersed Second Liquid Phase. Chem. Eng. Sci. **1986**, *41* (7), 1873–1877.
11. Mehra, A. Intensification of Multiphase Reactions through the Use of a Microphase-I. Theor. Chem. Eng. Sci. **1988**, *43* (4), 899–912.
12. Mehra, A.; Pandit, A.; Sharma, M.M. Intensification of Multiphase Reactions Through the Use of a Microphase-II. Expl. Chem. Eng. Sci. **1988**, *43* (4), 913–927.
13. Budavori, S. *The Merck Index*; 11th Ed.; Merck and Co.: New Jersey, 1989; pp. 3107, 3681, 9581.
14. Higbie, R. The Rate of Absorption of a Pure Gas into a Still Liquid During Short Periods of Exposure. Trans. Am. Inst. Chem. Eng. **1935**, *31*, 365–389.
15. Park, S.W.; Ryu, J.H.; Lee, S.S.; Hwang, K.S.; Kumazawa, H. Gas Absorption of CO_2 into Emulsion with Alkaline Aqueous Solution. Hwahak Konghak (Korea) **1997**, *35* (4), 476–484.
16. Yu, W.; Astarita, G.; Savage, D.W. Kinetics of Carbon Dioxide Absorption in Solutions of Methyldiethanolamine. Chem. Eng. Sci. **1985**, *40* (8), 1585–1590.
17. Hikita, H.; Asai, S.; Katsu, Y.; Ikuno, S. Absorption of Carbon Dioxide into Aqueous Monoethanolamine Solutions. AIChE. J. **1979**, *25* (5), 793–800.
18. Blanc, C.C.; Demarais, G. The Reaction Rate of CO_2 with Diethanolamine. Int. Chem.Eng. **1984**, *24* (1), 43–52.
19. Littel, R.J.; van Swaaij, W.P.M.; Versteeg, G.F. Kinetics of Carbon Dioxide with Tertiary Amines in Aqueous Solution. AIChE. J. **1990**, *36* (11), 1633–1640.
20. Danckwerts, P.V. *Gas–Liquid Reactions*; McGraw-Hill: New York, 1970; 15.

MARCEL DEKKER, INC.
270 Madison Avenue, New York, New York 10016

21. Danckwerts, P.V.; Sharma, M.M. The Absorption of Carbon Dioxide into Solutions of Alkalis and Amines. Chem. Eng. **1966**, *44*, 244–280.
22. Nijsing, R.A.T.O.; Hendriksz, R.H.; Kramers, H. Absorption of CO_2 in Jet and Falling Films of Electrolyte Solutions, with and without Chemical Reaction. Chem. Eng. Sci. **1959**, *10*, 88–104.
23. Wang, Y.W.; Xu, S.; Otto, F.D.; Mather, A.E. Solubility of N_2O in Alkanolamines and in Mixed Solvents. Chem. Eng. J. **1992**, *48*, 31–40.
24. Doraiswany, L.K.; Sharma, M.M. *Heterogeneous Reaction: Analysis, Example and Reactor Design*; Wiley: New York, 1984; Vol. 2, 17–26.

Received November 2000
Revised May 2001

MARCEL DEKKER, INC.
270 Madison Avenue, New York, New York 10016

Request Permission or Order Reprints Instantly!